Available online at www.sciencedirect.com
ScienceDirect
Mendeleev Commun., 2021, **31**, 163–165

Mendeleev Communications

# Solvent-free deposition of hybrid halide perovskites onto thin films of copper iodide p-type conductor

**Aleksei Yu. Grishko,[a] Elena A. Zharenova,[a] Eugene A. Goodilin[a,b,c] and Alexey B. Tarasov*[a,b]**

[a] *Department of Materials Science, M. V. Lomonosov Moscow State University, 119991 Moscow, Russian Federation. E-mail: alexey.bor.tarasov@yandex.ru*
[b] *Department of Chemistry, M. V. Lomonosov Moscow State University, 119991 Moscow, Russian Federation*
[c] *N. S. Kurnakov Institute of General and Inorganic Chemistry, Russian Academy of Sciences, 119991 Moscow, Russian Federation*

DOI: 10.1016/j.mencom.2021.03.006

**We demonstrate that a widely used inorganic hole-transporting material, copper iodide (CuI), gets dissolved if halide perovskites are deposited atop from solutions which compromises the fabrication of CuI/perovskite heterojunctions using these methods. On the contrary, solvent-free approaches allow for the retaining of the CuI layer under the halide perovskite film thus making this approach beneficial for the development of perovskite photovoltaics.**

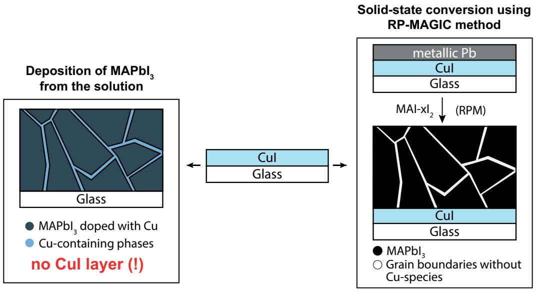

*Keywords*: hybrid materials, halide perovskites, inorganic semiconductors, p-type semiconductors, hole-transporting layers.

Perovskite solar cells based on organic–inorganic metal halide perovskites have recently attracted considerable attention because of their unbeatable cost–performance ratio. Perovskite solar cells can be made in regular (n-i-p) and inverted (p-i-n) configurations[1] comprising so-called 3D-perovskites, layered perovskites,[2,3] and related compounds.[4] Despite somewhat lower record power conversion efficiencies (PCEs) of p-i-n devices (22.3%)[5] compared to the n-i-p (25.2%)[6] architecture, they are considered as a more promising solution because they employ fully inorganic hole-transporting materials (HTMs) with a much better intrinsic chemical stability and lower cost.[7–9]

Solution processability is one of the most appealing features of halide perovskites; however, one has to ensure that no dissolution of the underlying layer occurs upon this deposition. This issue has been thoroughly addressed in organic electronics where orthogonal solvents are used for the deposition of multilayered structures.[10] However, little attention has been paid to the compliance of deposition of halide perovskites on top of inorganic HTMs from solutions. In particular, many reports on p-i-n perovskite solar cells claim to employ the CuI/MAPI (MAPI = $MeNH_3PbI_3$) heterojunction with quite high PCEs; however, they never actually confirmed that a thin film of CuI is retained in the device after perovskite deposition.[11–13]

In this work, we demonstrated that, due to similar chemical nature, copper iodide (CuI) is prone to dissolution in contact with a solution of halide perovskites, which compromises the fabrication of CuI/perovskite heterojunctions using a traditional solution-based approach. We also demonstrated that thin layers of CuI (~58 nm) are retained when a halide perovskite layer is deposited by a solvent-free deposition technique thus providing a path to the fabrication of devices based on CuI/halide perovskite heterojunctions.

The dissolution of a 0.3 M dispersion of CuI in pure DMSO and in 1.2 M solutions of MAI/$PbI_2$/MAPI in DMSO is shown in Figure S1 (Online Supplementary Materials). It is evident that copper iodide is poorly soluble in pure DMSO; however, the presence of 1.2 M MAI/$PbI_2$/MAPI greatly enhances its solubility. This behavior can be expected considering the ability of CuI to dissolve in the presence of an excess of $I^-$ ions and N-containing ligands such as $MeNH_3^+$.[14,15]

We confirmed the relevance of this model experiment to the actual deposition of halide perovskites from solution. First, reference films of MAPI and CuI were spin-coated on a glass substrate. X-ray diffraction (XRD) analysis showed that target phases were obtained and no impurities were present in the films (Figure 1). The CuI film exhibited a very pronounced texture with the only (111) reflection observed in the XRD pattern. The thickness of CuI films was estimated at 58 nm from the SEM images [Figure 1(*c*)].

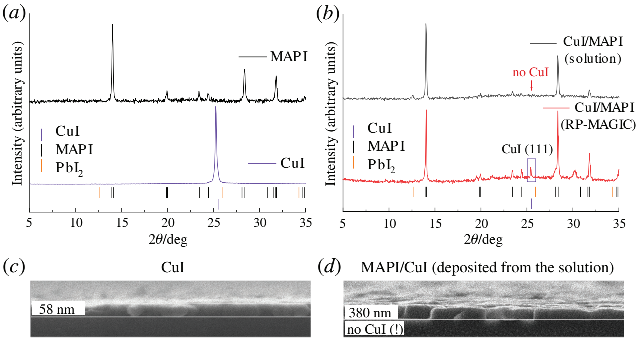

**Figure 1** XRD patterns of (*a*) pristine MAPI ($MeNH_3PbI_3$) and CuI films, (*b*) MAPI films deposited onto CuI from the solution in DMSO and using an RP-MAGIC approach; SEM cross-sections of (*c*) CuI and (*d*) MAPI films deposited from the solution on top of CuI films.

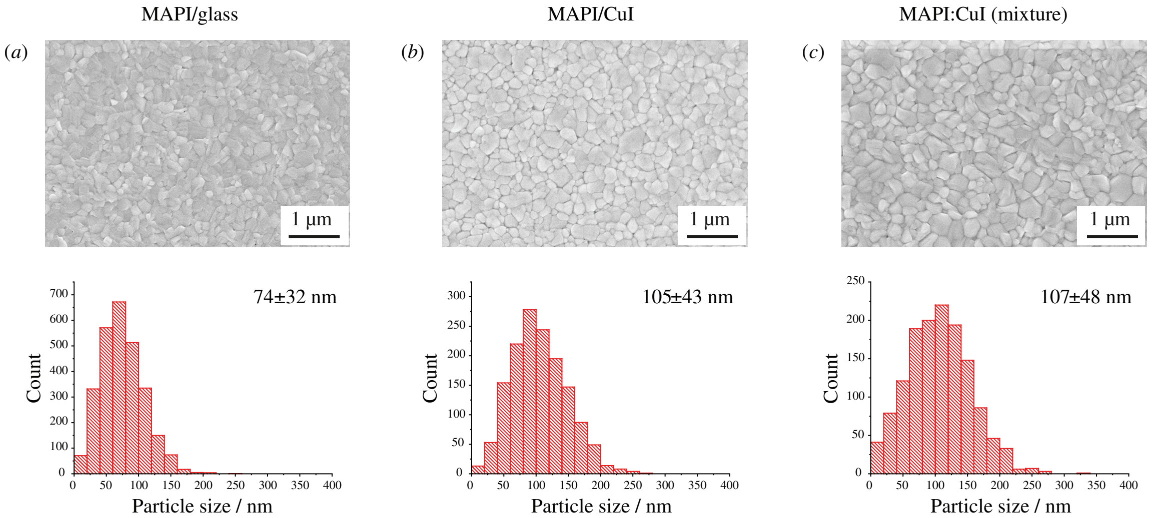

**Figure 2** SEM images of surface morphology of MAPI films obtained by the deposition of (*a*) a MAPI solution onto a glass substrate, (*b*) a MAPI solution onto a thin (58 nm) film of CuI, and (*c*) a MAPI solution containing 3 mol% CuI.

Next, we deposited a ~380 nm-thick MAPI film onto a CuI film by means of spin-coating using a 1.3 M stoichiometric solution in DMSO. The SEM images of the cross-section showed no sign of the CuI thin film suggesting that it was dissolved or delaminated during the deposition. The MAPI film deposited onto the CuI film exhibited a larger grain size [Figure 2(*b*)] compared to the one deposited onto a bare glass substrate [Figure 2(*a*)]. In order to clarify whether this effect was due to the presence of dissolved CuI in perovskite thin film or due to the fact that the CuI film itself (a very thin layer of CuI could remain on the substrate) guided the crystallization, we fabricated a reference sample using a solution containing MAPI and 1 mol% CuI [Figure 2(*c*)] and observed an increase in the average grain size in both the cases, which suggests that, upon a contact of the MAPI solution with the CuI film, the latter dissolved and Cu-related species guided the following crystallization process.

According to XRD data, the MAPI deposited on top of CuI exhibited no CuI-related reflection due to the dissolution of the underlying copper iodide layer or probable incorporation of CuI at the grain boundaries. Indeed, $Cu^+$ ions can be introduced into a halide perovskite lattice; however, based on the available data, this effect cannot be unambiguously assigned to either substitution at the $Pb^{2+}$ sites or its incorporation into interstitials.[16,17] Moreover, low concentrations of CuI can complicate the analysis of XRD data; thus, we performed a model solid-state synthesis in order to identify possible chemical transformations in the $MAPbI_3$–CuI system. Powder XRD of pellets containing different amounts of $MAPbI_3$ and CuI (5 and 15 mol%) sintered at 200 °C for 24 h exhibited additional reflections that cannot be assigned to $MAPbI_3$, $PbI_2$, CuI or $MACu_2I_3$ phases[18] (Figure S2). The available data do not allow one to identify these reflections and ascribe them to Cu-doped halide perovskite or other phases; however, it can be clearly seen that a chemical reaction occurs under these conditions.

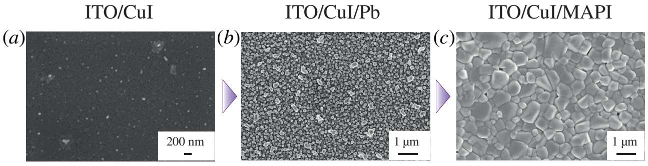

**Figure 3** SEM images of thin films: (*a*) ITO/CuI, (*b*) ITO/CuI/Pb, and (*c*) ITO/CuI/MAPI; Pb was converted into MAPI using an RP-MAGIC approach.

We note that high efficiencies obtained using the solution-based deposition of halide perovskite on top of thin CuI films that we expect to undergo dissolution are not surprising. There are a few reports on HTL-/ETL-free (hole-transporting layer/electron-transporting layer) perovskite solar cells, which demonstrate that moderate efficiencies can be obtained with just one charge-selective contact.[19] It is believed that high diffusion lengths characteristic of halide perovskite materials combined with appropriate charge-blocking contacts (hole-blocking at the ETL side for HTL-free and electron-blocking at the HTL side for ETL-free solar cells) are responsible for these unexpectedly high PCEs.

In order to avoid the destruction of underlying CuI layer, we employed the solvent-free deposition technique to make a CuI/MAPI stack following the RP-MAGIC approach.[20] For this purpose, a thin film of metallic lead was evaporated on top of a glass/CuI thin film and converted into MAPI using reactive polyiodide melts (see Figure 3 and Online Supplementary Materials for details). We note that, although thermal evaporation of metallic lead results in a rough film with lots of voids between individual Pb particles, the final perovskite film is smooth and void-free. The XRD data [Figure 1(*b*)] clearly show that a CuI reflection is present in this sample, which rejects the hypothesis that the absence of CuI reflection in the sample obtained using a solution-based method is due to signal attenuation, and it finally verifies that CuI thin films get dissolved upon direct contact with the MAPI solution. Note that the dissolution of CuI upon MAPI deposition from solution can be the reason that some authors reported on the formation of deep defect states in CuI/MAPI devices.[13]

Thus, we have shown that the CuI/MAPI heterojunction cannot be obtained using the solution–deposition of MAPI without the intermixing of constituting layers. On the other hand, solvent-free deposition methods pave the reliable way to fabricate this kind of interfaces for the development of perovskite photovoltaics.

This study was supported by the Russian Foundation for Basic Research and the Moscow City Government (project no. 19-33-70077).

*Online Supplementary Materials*

Supplementary data associated with this article can be found in the online version at doi: 10.1016/j.mencom.2021.03.006.

## References

1 J.-P. Correa-Baena, A. Abate, M. Saliba, W. Tress, T. J. Jacobsson, M. Grätzel and A. Hagfeldt, *Energy Environ. Sci.*, 2017, **10**, 710.

2 D. H. Cao, C. C. Stoumpos, O. K. Farha, J. T. Hupp and M. G. Kanatzidis, *J. Am. Chem. Soc.*, 2015, **137**, 7843.

3 E. I. Marchenko, S. A. Fateev, A. A. Petrov, E. A. Goodilin and A. B. Tarasov, *Mendeleev Commun.*, 2020, **30**, 279.

4 W. Li, Z. Wang, F. Deschler, S. Gao, R. H. Friend and A. K. Cheetham, *Nat. Rev. Mater.*, 2017, **2**, 16099.

5 X. Zheng, Y. Hou, C. Bao, J. Yin, F. Yuan, Z. Huang, K. Song, J. Liu, J. Troughton, N. Gasparini, C. Zhou, Y. Lin, D. J. Xue, B. Chen, A. K. Johnston, N. Wei, M. N. Hedhili, M. Wei, A. Y. Alsalloum, P. Maity, B. Turedi, C. Yang, D. Baran, T. D. Anthopoulos, Y. Han, Z. H. Lu, O. F. Mohammed, F. Gao, E. H. Sargent and O. M. Bakr, *Nat. Energy*, 2020, **5**, 131.

6 *NREL, Best Research-Cell Efficiency Chart*, https://www.nrel.gov/pv/assets/pdfs/best-research-cell-efficiencies.20190802.pdf.

7 Z. Yu and L. Sun, *Small Methods*, 2018, **2**, 1700280.

8 J. Chen and N.-G. Park, *J. Phys. Chem. C*, 2018, **122**, 14039.

9 N. N. Shlenskaya, A. S. Tutantsev, N. A. Belich, E. A. Goodilin, M. Grätzel and A. B. Tarasov, *Mendeleev Commun.*, 2018, **28**, 378.

10 A. M. Gaikwad, Y. Khan, A. E. Ostfeld, S. Pandya, S. Abraham and A. C. Arias, *Org. Electron.*, 2016, **30**, 18.

11 W. Sun, S. Ye, H. Rao, Y. Li, Z. Liu, L. Xiao, Z. Chen, Z. Bian and C. Huang, *Nanoscale*, 2016, **8**, 15954.

12 H. Wang, Z. Yu, X. Jiang, J. Li, B. Cai, X. Yang and L. Sun, *Energy Technol.*, 2017, **5**, 1836.

13 D. B. Khadka, Y. Shirai, M. Yanagida and K. Miyano, *Sol. Energy Mater. Sol. Cells*, 2020, **210**, 110486.

14 P. Atkins,T. Overton, J. Rourke, M. Weller and F. Armstrong, *Shriver and Atkins' Inorganic Chemistry*, 5th edn., Oxford University Press, USA, 2010.

15 R. R. Conry, *Copper: Inorganic & Coordination Chemistry*, Wiley Online Library, 2011.

16 Y. Shirahata and T. Oku, *Phys. Status Solidi*, 2017, **214**, 1700268.

17 M. Abdi-Jalebi, M. Pazoki, B. Philippe, M. I. Dar, M. Alsari, A. Sadhanala, G. Divitini, R. Imani, S. Lilliu, J. Kullgren, H. Rensmo, M. Grätzel and R. H. Friend, *ACS Nano*, 2018, **12**, 7301.

18 A. A. Petrov, V. N. Khrustalev, Ya. V. Zubavichus, P. V. Dorovatovskii, E. A. Goodilin and A. B. Tarasov, *Mendeleev Commun.*, 2018, **28**, 245.

19 N. Kumari, S. R. Patel and J. V Gohel, *Rev. Adv. Mater. Sci.*, 2018, **53**, 161.

20 I. Turkevych, S. Kazaoui, N. A. Belich, A. Y. Grishko, S. A. Fateev, A. A. Petrov, T. Urano, S. Aramaki, S. Kosar, M. Kondo, E. A. Goodilin, M. Graetzel and A. B. Tarasov, *Nat. Nanotechnol.*, 2019, **14**, 57.

*Received: 26th November 2020; Com. 20/6377*